Special Conference Edition, April, 2022 http://dx.doi.org/10.4314/bajopas.v13i1.67S
Bayero Journal of Pure and Applied Sciences, 13(1): 439 - 446
ISSN 2006 – 6996

INVESTIGATING TURING PATTERNS IN CANCER-IMMUNE CELLS INTERACTION MODEL

Oluwatosin, O., Ibrahim, A. K. and Hussaini, N.*
Department of Mathematical Sciences, Bayero University Kano, P.M.B. 3011, Kano, Nigeria.
*Corresponding author. Email: nhussaini.mth@buk.edu.ng

ABSTRACT
Pattern formation is very broad in nature, and understanding the causes of its generation has greatly advanced over the past decades. In this paper, we investigate Turing pattern formation in a cancer-immune cells interaction which is spatially distributed. We derived conditions under which Turing patterns emerged due to diffusion-driven instability. Numerical results revealed the formation of isolated groups such as spotted and stripe-like patterns due to the cells interaction. Furthermore, the results have shown that the model exhibited patterns due to cross-diffusion.
Keywords: Cancer cells; Immune cells; Reaction Diffusion; Turing pattern; Cross-Diffusion; Bendixson-Dulac criterion.

INTRODUCTION

Cancer is one of the leading causes of death worldwide, accounting for an estimated 10 million deaths in 2020 (WHO, 2021). It has been projected that by 2030, cancer will surpass heart disease as the leading cause of death in some countries like Australia, Canada, the UK, New Zealand, and Denmark (Wishart, 2015). It is a disease that begins when the body has lost control of the cells or due to damages or defects in genes involved in cell division which is the rapid creation of abnormal cells that grow beyond their usual boundaries; a process referred to as metastasis. During metastasis, disseminating cancer cells escape from primary tumors and acquire cellular traits that allow them to travel and colonize distant organs (Chambers & Werb, 2015). Understanding the mechanism of cancer progression is necessary for its diagnosis and treatment, thus researchers have developed mathematical models to understand and predict how cancer cells evolve and respond to therapy (Lingeshwaran & Puthur, 2018). According to Byrne (1999a), to develop an effective cancer treatment, it is important to identify the mechanisms controlling cancer growth. The interactions between tumor cells and other components of the tumor micro-environment such as immune cells, fibroblasts, and other connective tissue cells are complex and continuously changing because interaction strengths are density-dependent. Consequently, understanding these interactions sufficiently to derive cancer immunotherapies (e.g., vaccines), has proven a very challenging task (Gajewski, 2007). In the area of developmental Biology, partial differential equations for pattern formation usually take the form of reaction-diffusion type (Turing, 1952). The effect which diffusion has on pattern formation in reaction-diffusion systems has been discussed by Turing (1952). Since then, more attention has been paid to theoretical models to explain pattern formation in many areas especially Biology (Zheng & Jianwei, 2014). It is pertinent to note that for a two-component reaction-diffusion system, a key requirement for diffusion-driven instability is the concept of long-range inhibition and short-range activation (Gierer & Meinhardt, 1972).

In this paper, we modified the model presented by Wilkie and Hahnfeldt (2013) by adding diffusion. We further assumed cancer and immune cells sub-populations to be governed by Gompertzian growth function.

Growth processes have often been characterized by a sigmoidal curve reflecting an initial relatively slow growth rate, increasing to a maximum and then slowing down to approach an upper limit. It has frequently been used to describe growth in size across time. The most common mathematical forms used to model human size as a function of age include the logistic and the Gompertz curves. The Logistic curve, however, locates the point of inflection in terms of maximum growth rate exactly half-way between the initial and final size and the rate is imputed as symmetrical on either side of this. However, limiting feature of the logistic curve is that the location of the point of inflection in terms of maximum growth rate is exactly half-way between the initial and final size and the rate is imputed as symmetrical on either side of the midpoint (Michelle, 2012).

The Gompertzian equation originated from the actuarial model developed by Gompertz (Gompertz, 1825), and was applied to the study of growth in biological and economic contexts in 1932. Laird (1964) showed that the Gompertzian equation could describe the normal growth of an organism such as the guinea pig over an incredible 10 000-fold range of growth because of the equation's ability to exhibit exponential retardation-a feature not incorporated in other growth equations used in biological contexts at that time such as the logistic equation.

Researchers have fitted the Gompertz growth function to different models such as plant growth, bird growth, fish growth, and growth of other animals, to tumour growth and bacterial growth (Tjørve & Tjørve, 2017).

This paper is organized as follows. In Section 2, we formulate the model with some stability analysis. Results and discussion are reported in Section 3.

MODEL FORMULATION

The Gompertz model is one of the most frequently used sigmoid models fitted to growth data and other data, perhaps only second to the logistic model (Tjørve & Tjørve, 2017). Researchers have fitted the Gompertz model to different growth data sets from plant, bird, fish, and other animals, to tumor and bacterial growths (Tjørve & Tjørve, 2017) and was found to fit data more accurately. We consider two populations of cells namely cancer cells, $C(t)$, and immune cells, $I(t)$. Cancer and immune cells are assumed to grow according to a Gompertz growth function. Thus, we consider the model:

$$\left.\begin{aligned}\frac{\partial}{\partial t}C(x,t) &= \alpha C\ln\left(\frac{K_C}{C}\right) - a_0 CI + d_{11}^G \Delta C + d_{12}^G \Delta I,\\ \frac{\partial}{\partial t}I(x,t) &= \gamma(\rho C + I)\ln\left(\frac{K_I}{I}\right) + d_{21}^G \Delta C + d_{22}^G \Delta I\end{aligned}\right\} \quad (2.1)$$

$$C(0) = C_0, \qquad I(o) = I_0,$$

$$\alpha, K_C, a_0, \gamma, \rho, K_I > 0.$$

where α is cancer proliferation rate, γ is immune proliferation rate, a_0 is predation strength, ρ is cancer infection rate, K_C is cancer carrying capacity, K_I is immune carrying capacity, the positive constants d_{11}^G, d_{22}^G are the self-diffusion coefficients and d_{12}^G, d_{21}^G are called the cross-diffusion coefficients, which imply that one-species molecules tend to diffuse along the direction of lower concentration of the other specie molecules. $\Delta = \frac{\partial^2}{\partial x^2} + \frac{\partial^2}{\partial y^2}$ is the Laplacian operator in the two-dimensional space, which describes the random movement of molecules in the cell.

Existence of Equilibrium Points

In this section, we establish the existence of the equilibrium points of the system. By equating the non-spatial part of system (2.1) to zero, we find that the system has 4 possible nonnegative equilibria, namely $E_0^G(0,0)$, $E_1^G(K_C,0)$, $E_2^G(0,K_I)$ and the co-existence equilibrium $E_3^G\left(\frac{K_C}{e^{\frac{a_0 K_I}{\alpha}}}, K_I\right)$. $E_0^G(0,0)$ is trivial as both the cancer and immune cells are absent. $E_1^G(K_C,0)$ corresponds to zero immune presence, $E_2^G(0,K_I)$ corresponds to zero cancer presence and $E_3^G\left(\frac{K_C}{e^{\frac{a_0 K_I}{\alpha}}}, K_I\right)$ corresponds to a state allowing both the cancer and immune cells to co-exist. The focus of our analysis will be on the co-existence of the cancer and immune cells given by

$$E_3^G = \left(\frac{K_C}{e^{\frac{K_I a_0}{\alpha}}}, K_I\right). \quad (2.2)$$

Local Stability Analysis without Diffusion

In this section, to show the Turing mechanism of how patterns are formed (Turing instability), we establish the local stability analysis for steady-state and seek conditions on the emergence of Turing patterns.

Theorem 2.1 *The positive co-existence equilibrium point (2.2) of the system (2.1) (without cross-diffusion) is locally asymptotically stable.*

Proof. Note that the Jacobian matrix for the system of equation (2.1) is

$$J^G = \begin{pmatrix} \alpha\ln\left(\frac{K_C}{C}\right) - \alpha - a_0 I & -a_0 C \\ \gamma\rho\ln\left(\frac{K_I}{I}\right) & \gamma\ln\left(\frac{K_I}{I}\right) - \frac{\gamma(C\rho+I)}{I} \end{pmatrix}$$

Evaluating the Jacobian matrix at the positive co-existence equilibrium (2.2), we get

$$J^G(E_3^G) = \begin{bmatrix} -\alpha & -\frac{a_0 K_C}{e^{\frac{K_I a_0}{\alpha}}} \\ 0 & -\frac{\gamma\left(\frac{\rho K_C}{e^{\frac{K_I a_0}{\alpha}}} + K_I\right)}{K_I} \end{bmatrix} \tag{2.3}$$

where,

$$J_{11}^G = -\alpha \tag{2.4}$$

$$J_{12}^G = -\frac{a_0 K_C}{e^{\frac{K_I a_0}{\alpha}}} \tag{2.5}$$

$$J_{21}^G = 0 \tag{2.6}$$

$$J_{22}^G = -\frac{\gamma\left(\frac{\rho K_C}{e^{\frac{K_I a_0}{\alpha}}} + K_I\right)}{K_I} \tag{2.7}$$

The local stability for system (2.1) exist since we have

$$tr(J^G) < 0 \tag{2.8}$$

$$det(J^G) > 0 \tag{2.9}$$

Hence, since (2.8) and (2.9) are satisfied for (2.3), then the positive equilibrium points of the system are said to be locally asymptotically stable.

Local Stability Analysis with Self-Diffusion

For the local stability analysis with self-diffusion, the spatial model (2.1) is reduced to the following standard R-D equations

$$\begin{aligned} \frac{\partial}{\partial t} C(x,t) &= \alpha C \ln\left(\frac{K_C}{C}\right) - a_0 CI + d_{11}^L \Delta C, \\ \frac{\partial}{\partial t} I(x,t) &= \gamma(C\rho + I)\ln\left(\frac{K_I}{I}\right) + d_{22}^L \Delta I \end{aligned} \tag{2.10}$$

For this simplified model, we can prove:

Theorem 2.2 *The positive steady state E_3^G of (2.10) is locally asymptotically stable.*

Proof. At the positive steady state E_3^G, the linearization of equation (2.10) is

$$\begin{aligned} \frac{\partial}{\partial t} C(x,t) &= J_{11}^G C + J_{12}^G I + d_{11}^G \Delta C, \\ \frac{\partial}{\partial t} I(x,t) &= J_{21}^G C + J_{22}^G I + d_{22}^G \Delta I \end{aligned} \tag{2.11}$$

Following Malchow et al. (2008), any solution of (2.11) can be expanded into Fourier series so that

$$\left.\begin{aligned} C(x,t) &= \sum_{n,m=0}^{\infty} C_{nm}(x,t) = \sum_{n,m=0}^{\infty} \alpha_{n,m}(t)\sin Kx \\ I(x,t) &= \sum_{n,m=0}^{\infty} I_{nm}(x,t) = \sum_{n,m=0}^{\infty} \beta_{n,m}(t)\sin Kx \end{aligned}\right\} \tag{2.12}$$

where $0 < x < L_x$ and $0 < y < L_y$ L_x and L_y giving the size of the system in the directions of x and y respectively. $K = (k_n, k_m)$ where $k_n = \pi n/L_x$ and $k_m = \pi m/L_y$ are the corresponding wavenumbers.

Using system (2.12), system (2.11) becomes

$$\begin{aligned} \frac{d}{dt}\alpha_{n,m}\sin Kx &= d_{11}^G \Delta\left(\alpha_{n,m}(t)\sin Kx\right) + J_{11}^G\left(\alpha_{n,m}(t)\sin Kx\right) + \\ &\quad J_{12}^G\left(\beta_{n,m}(t)\sin Kx\right) \\ \frac{d}{dt}\beta_{n,m}\sin Kx &= d_{22}^G \Delta\left(\beta_{n,m}(t)\sin Kx\right) + J_{21}^G\left(\alpha_{n,m}(t)\sin Kx\right) + \\ &\quad J_{22}^G\left(\beta_{n,m}(t)\sin Kx\right) \end{aligned}$$

$$\frac{d}{dt}\alpha_{n,m}\sin Kx = -d_{11}^G K^2 \alpha_{n,m}\sin Kx + J_{11}^G \alpha_{n,m}\sin Kx + J_{12}^G \beta_{n,m}\sin Kx$$

$$\frac{d}{dt}\beta_{n,m}\sin Kx = -d_{22}^{G}K^2\beta_{n,m}\sin Kx + J_{21}^{G}\alpha_{n,m}\sin Kx + J_{22}^{G}\beta_{n,m}\sin Kx$$

$$\left.\begin{aligned}\frac{d}{dt}\alpha_{n,m} &= -d_{11}^{G}K^2\alpha_{n,m} + J_{11}^{G}\alpha_{n,m} + J_{12}^{G}\beta_{n,m}\\ \frac{d}{dt}\beta_{n,m} &= -d_{22}^{G}K^2\beta_{n,m} + J_{21}^{G}\alpha_{n,m} + J_{22}^{G}\beta_{n,m}\end{aligned}\right\} \tag{2.13}$$

$$\frac{d}{dt}\begin{pmatrix}\alpha_{n,m}\\ \beta_{n,m}\end{pmatrix} = \begin{pmatrix}J_{11}^{G} - d_{11}^{G}K^2 & J_{12}^{G}\\ J_{21}^{G} & J_{22}^{G} - d_{22}^{G}K^2\end{pmatrix}\begin{pmatrix}\alpha_{n,m}\\ \beta_{n,m}\end{pmatrix} \tag{2.14}$$

A general solution of (2.13) has the form $C_a e^{\lambda_1 t} + C_b e^{\lambda_2 t}$, where the constants C_a and C_b are determined by the initial conditions and the exponents $\lambda_{1,2}$ are the eigenvalues of the following matrix:

$$\bar{M}^{G} = \begin{pmatrix}J_{11}^{G} - d_{11}^{G}K^2 & J_{12}^{G}\\ J_{21}^{G} & J_{22}^{G} - d_{22}^{G}K^2\end{pmatrix} \tag{2.15}$$

$$D^{G} = \begin{pmatrix}d_{11}^{G} & 0\\ 0 & d_{22}^{G}\end{pmatrix}$$

where D^{G} are the entries for the self-diffusion coefficients.
The eigenvalues $\lambda_{1,2}$ of (2.15) satisfy the following characteristics polynomial

$$\lambda^2 - m\lambda + n = 0 \tag{2.16}$$

where

$$\begin{aligned}m = tr(\bar{M}^{G}) &= J_{11}^{G} - d_{11}^{G}K^2 + J_{22}^{G} - d_{22}^{G}K^2\\ &= -d_{k}^{G}11K^2 - d_{22}^{G}K^2 + J_{11}^{G} + J_{22}^{G}\\ &= -(d_{11}^{G} + d_{22}^{G})K^2 + (J_{11}^{G} + J_{22}^{G})\\ &= -(d_{11}^{G} + d_{22}^{G})K^2 + tr(J^{G}) < 0\end{aligned}$$

Therefore, $tr(\bar{M}^{G}) < 0$ where $d_{11}^{G},\ d_{22}^{G} \in \mathbb{R}^{+}$.

$$\begin{aligned}n = det(\bar{M}^{G}) &= (J_{11}^{G} - d_{11}^{G}K^2)(J_{22}^{G} - d_{2}^{G}K^2) - J_{11}^{G}J_{22}^{G}\\ &= J_{11}^{G}J_{22}^{G} - J_{11}^{G}d_{22}^{G}K^2 - J_{22}^{G}d_{11}^{G}K^2 + d_{11}^{G}d_{22}^{G}K^4 - J_{11}^{G}J_{22}^{G}\\ &= det(D^{G})K^4 - (J_{11}^{G}d_{22}^{G} + J_{22}^{G}d_{11}^{G})K^2 + det(J^{G}) > 0\end{aligned}$$

$det(D^{G}),\ det(J^{G}),\ d_{11}^{G},\ d_{22}^{G} > 0$ and $J_{11}^{G},\ J_{22}^{G} < 0$. Therefore, $det(\bar{M}^{G}) > 0$.
Thus, we have $tr(\bar{M}^{G}) < 0 < det(\bar{M}^{G})$. Hence, the proof is completed.

Local Stability Analysis with Self-Diffusion and Cross-Diffusion

For the local stability analysis with self-diffusion and cross-diffusion, the general representation of the linearized form of (2.1) about (2.2) is as follows:

$$\left.\begin{aligned}\frac{\partial}{\partial t}C(x,t) &= d_{11}^{G}\Delta C + d_{12}^{G}\Delta I + J_{11}^{G}C + J_{12}^{G}I\\ \frac{\partial}{\partial t}I(x,t) &= d_{21}^{G}\Delta C + d_{22}^{G}\Delta I + J_{21}^{G}C + J_{22}^{G}I\end{aligned}\right\} \tag{2.17}$$

$$D^{G} = \begin{bmatrix}d_{11}^{G} & d_{12}^{G}\\ d_{21}^{G} & d_{22}^{G}\end{bmatrix}, \quad J^{G} = \begin{bmatrix}J_{11}^{G} & J_{12}^{G}\\ J_{21}^{G} & J_{22}^{G}\end{bmatrix}, \quad U = \begin{bmatrix}C\\ I\end{bmatrix}$$

where

d_{11}^{G}, d_{22}^{G} are the self − diffusion coefficients

d_{12}^{G}, d_{21}^{G} are the cross − diffusion coefficients

$J_{i,j}, i, j = 1,2$ are the cofactors of the linearized Jacobian matrix

Using system (2.12), system (2.17) becomes

$$\frac{d}{dt}\alpha_{n,m}\sin Kx = d_{11}^G\Delta\left(\alpha_{n,m}(t)\sin Kx\right) + d_{12}^G\Delta\left(\beta_{n,m}(t)\sin Kx\right) + J_{11}^G\left(\alpha_{n,m}(t)\sin Kx\right) + J_{12}^G\left(\beta_{n,m}(t)\sin Kx\right)$$
$$\frac{d}{dt}\beta_{n,m}\sin Kx = d_{21}^G\Delta\left(\alpha_{n,m}(t)\sin Kx\right) + d_{22}^G\Delta\left(\beta_{n,m}(t)\sin Kx\right) + J_{21}^G\left(\alpha_{n,m}(t)\sin Kx\right) + J_{22}^G\left(\beta_{n,m}(t)\sin Kx\right)$$

$$\frac{d}{dt}\alpha_{n,m} = -d_{11}^G K^2\alpha_{n,m} - d_{12}^G K^2\beta_{n,m} + J_{11}^G\alpha_{n,m} + J_{12}^G\beta_{n,m}$$
$$\frac{d}{dt}\beta_{n,m} = -d_{21}^G K^2\alpha_{n,m} - d_{22}^G K^2\beta_{n,m} + J_{21}^G\alpha_{n,m} + J_{22}^G\beta_{n,m}$$
$$\frac{d}{dt}\begin{pmatrix}\alpha_{n,m}\\ \beta_{n,m}\end{pmatrix} = \begin{pmatrix}J_{11}^G - d_{11}^G K^2 & J_{12}^G - d_{12}^G K^2\\ J_{21}^G - d_{21}^G K^2 & J_{22}^G - d_{22}^G K^2\end{pmatrix}\begin{pmatrix}\alpha_{n,m}\\ \beta_{n,m}\end{pmatrix}$$

$$\bar{N}^G = \begin{pmatrix}J_{11}^G - d_{11}^G K^2 & J_{12}^G - d_{12}^G K^2\\ J_{21}^G - d_{21}^G K^2 & J_{22}^G - d_{22}^G K^2\end{pmatrix}$$
$$\kappa^G = \begin{pmatrix}d_{11}^G & d_{12}^G\\ d_{21}^G & d_{22}^G\end{pmatrix}$$

where κ^G are the entries for the self-diffusion and cross-diffusion coefficients.

$$tr(\bar{N}^G) = J_{11}^G - d_{11}^G K^2 + J_{22}^G - d_{22}^G K^2 = -(d_{11}^G + d_{22}^G)K^2 + tr(J^G) < 0$$

$$det(\bar{N}^G) = (J_{11}^G - d_{11}^G K^2)(J_{22}^G - d_2^G K^2) - (J_{21}^G - d_{21}^G K^2)(J_{12}^G - d_{12}^G K^2) = det(\kappa^G)K^4 - (J_{11}^G d_{22}^G + J_{22}^G d_{11}^G - J_{21}^G d_{12}^G - J_{12}^G d_{21}^G)K^2 + det(J^G)$$

Diffusive instability occurs when at least one of the following conditions is true

$$tr(\bar{N}^G) = -(d_{11}^G + d_{22}^G)K^2 + tr(J^G) > 0 \quad (2.18)$$

$$det(\bar{N}^G) = det(\kappa^G)K^4 - (J_{11}^G d_{22}^G + J_{22}^G d_{11}^G - J_{21}^G d_{12}^G - J_{12}^G d_{21}^G)K^2 + det(J^G) < 0 \quad (2.19)$$

The first condition will not be satisfied since $d_{11}^G, d_{22}^G \in \mathbb{R}^+$ and by (2.8), $tr(\bar{N}^G) < 0$.
Thus if we want the system to become unstable, we need (2.19) to be true. We look for $K > K_{min}$ where K_{min} is the first mode that can cause instability, i.e.
Let $P = K^2$, then

$$h(\mathrm{P}) = det(\kappa^G)P^2 - (J_{11}^G d_{22}^G + J_{22}^G d_{11}^G - J_{21}^G d_{12}^G - J_{12}^G d_{21}^G)P \quad + \quad det(J^G) < 0 \quad (2.20)$$

Now equation (2.20) will be quadratic in P which is a parabola that opens up since $det(\kappa^G)$ is positive. To find the minimum value of $h(P)$, we set the derivative with respect to P equal to zero:

$$\frac{dh(P)}{dP} = 2det(\kappa^G)P - (J_{11}^G d_{22}^G + J_{22}^G d_{11}^G - J_{21}^G d_{12}^G - J_{12}^G d_{21}^G) = 0$$

or

$$K_c^2 = \frac{J_{11}^G d_{22}^G + J_{22}^G d_{11}^G - J_{21}^G d_{12}^G - J_{12}^G d_{21}^G}{2det(\kappa^G)}$$

To find the minimum value, substitute this expression for P into (2.20).

$$\Rightarrow det(\kappa^G)\left[\frac{J_{11}^G d_{22}^G + J_{22}^G d_{11}^G - J_{21}^G d_{12}^G - J_{12}^G d_{21}^G}{2det(\kappa^G)}\right]^2 - (J_{11}^G d_{22}^G + J_{22}^G d_{11}^G - J_{21}^G d_{12}^G - J_{12}^G d_{21}^G)\left[\frac{J_{11}^G d_{22}^G + J_{22}^G d_{11}^G - J_{21}^G d_{12}^G - J_{12}^G d_{21}^G}{2det(\kappa^G)}\right] + det(J^G) < 0$$
$$\Rightarrow \quad J_{11}^G d_{22}^G + J_{22}^G d_{11}^G - J_{21}^G d_{12}^G - J_{12}^G d_{21}^G > 2\sqrt{det(\kappa^G)det(J^G)}$$

Hence for Turing instability to occur, the following conditions must be satisfied

$$tr(J^G) < 0 \quad (2.21)$$
$$det(J^G) > 0 \quad (2.22)$$
$$J_{11}^G d_{22}^G + J_{22}^G d_{11}^G - J_{21}^G d_{12}^G - J_{12}^G d_{21}^G > 0 \quad (2.23)$$
$$J_{11}^G d_{22}^G + J_{22}^G d_{11}^G - J_{21}^G d_{12}^G - J_{12}^G d_{21}^G > 2\sqrt{det(\kappa^G)det(J^G)} \quad (2.24)$$

Remark 2.1 *In the absence of cross-diffusion, the system (2.17) is stable as it satisfies the stability conditions (2.21) and (2.22). This will hold for any positive value of* d_{11}^G *and* d_{22}^G.

Remark 2.2 *With self-diffusion, the RD system is stable as it satisfies the stability conditions (2.21) and (2.22) being that the second term of* $det(\bar{M}^G)$ *will be positive as* $J_{11}^G, J_{22}^G < 0$ *(2.4 and 2.7) and* $d_{11}^G, d_{22}^G > 0$. *Therefore,* $det(\bar{M}^G)$ *will always be positive for all* $d_{11}^G, d_{22}^G \in \mathbb{R}^+$.

Remark 2.3 *With self-diffusion and cross-diffusion, the RD system needs to satisfy the conditions for Turing instability to hold. The trace* $tr(\bar{N}^G)$ *will remain negative but the determinant* $det(\bar{N}^G)$ *is uncertain. Hence we proceeded to show the sufficient conditions for* $det(\bar{N}^G) < 0$ *to hold which resulted to conditions (2.23) and (2.24).*

Global Stability Analysis

Theorem 2.3 *Suppose* $\Phi_w(C, I) = \frac{1}{CI}$ *is a Dulac function, then the system (2.1) is globally asymptotically stable.*

Proof. Define Dulac function

$$\Phi(C, I) = \frac{1}{CI} \qquad C, I > 0,$$

and denote the right-hand side of system (2.1) by $\Theta(C, I)$, $\Psi(C, I)$. We have

$$\begin{aligned} div(\Phi\Theta, \Phi\Psi) &= \frac{\partial \Phi\Theta}{\partial C} + \frac{\partial \Phi\Psi}{\partial I} \\ &= \frac{\partial}{\partial C}\left[\frac{1}{CI}\left(\alpha C \ln\left(\frac{K_C}{C}\right) - a_0 CI\right)\right] \\ &\quad + \frac{\partial}{\partial I}\left[\frac{1}{CI}\left(\gamma(C\rho + I)\ln\left(\frac{K_I}{I}\right)\right)\right] \\ &= -\frac{(\alpha+\gamma)}{CI} - \frac{\gamma\rho(1+\ln(\frac{K_I}{I}))}{I^2} < 0 \end{aligned}$$

Thus, system (2.1) does not have limit circle in Ω and by Bendixson-Dulac's criterion, the positive equilibrium points of the system (2.1) is globally asymptotically stable.

RESULTS AND DISCUSSION

In this paper, we consider a zero-flux boundary condition with region defined as a square, then we discretize the space and time in which the square is divided as $M \times N$ lattice site domain with h length of lattices and time step ht. The system size is set at 100×100 with time step $1/1000$ and space stepsize $x_{max} = 1/100$. We study the spatiotemporal dynamics of a cancer-immune cell interaction model with cross-diffusion under the zero-flux boundary conditions. We show that the Turing instability can be induced by cross-diffusion, which shows that the model dynamics portray patterns controlled by the diffusion coefficients. As one of our objectives is to investigate the influence of cross-diffusion on the cancer-immune model, the value of the cross-diffusion coefficients maybe positive, negative, or zero. The term positive cross-diffusion coefficient denotes the movement of the species in the direction of lower concentration of another species and negative cross-diffusion coefficient denotes that one species tends to diffuse in the direction of higher concentration (Gui-Quan, 2012).

We simulated the model using the parameter values given in Table (1) and ensured all the Turing conditions were satisfied.

Table 1: Parameter values and description

Parameters	Description	Values	Reference
α	Cancer proliferation rate	0.2	Wilkie and Hahnfeldt (2013)
γ	Immune proliferation rate	0.00002	Assumed
a_0	Predation strength	0.0001	Wilkie and Hahnfeldt (2013)
ρ	Cancer infection rate	1.5	Assumed
K_C	Cancer carrying capacity	100	Assumed
K_I	Immune carrying capacity	100	Assumed
d_{11}	Self-diffusion coefficient	50	Assumed
d_{12}	Cross diffusion coefficient	-1	Assumed
d_{21}	Cross diffusion coefficient	7000	Assumed
d_{22}	Self-diffusion coefficient	50	Assumed

In the numerical simulations, different types of dynamics were observed. The patterns generated show that the distribution and interaction of morphogens are caused by diffusion. The shade of the color represents the concentration of morphogen protein in the cells and it is found that the red corresponds to high, and blue corresponds to the low concentrations of cancer and immune cells respectively.

In Figures 1 and 2, spot patterns were observed in the immune cell population compared to the cancer cell population. There are more morphogen concentrations in the immune cells population when compared to the cancer cells population. In Figure 3, we observed a significant change in the patterns formed. Here, the cancer cross-diffusion coefficient is -2, which means there is more diffusion to an area of higher concentration while we have the immune cross-diffusion coefficient to tend to diffuse more to an area of lower concentration.

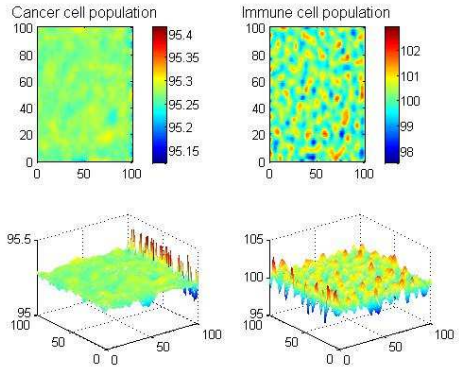

Figure 1: **Turing Patterns of cancer-immune model with Gompertzian growth (2.1) for $d_{11} = 50, d_{12} = -1, d_{21} = 7000, d_{22} = 50, \delta = 0.3$**

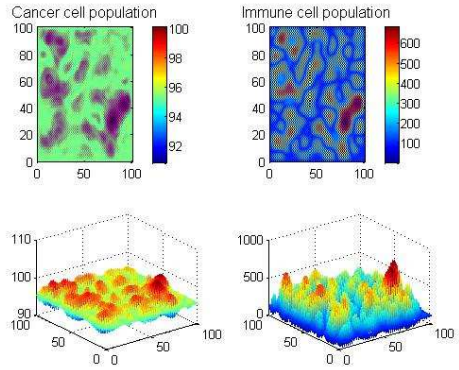

Figure 2: **Turing Patterns of cancer-immune model with Gompertzian growth (2.1) for $d_{11} = 200, d_{12} = -2, d_{21} = 7500, d_{22} = 200, \delta = 0.3$**

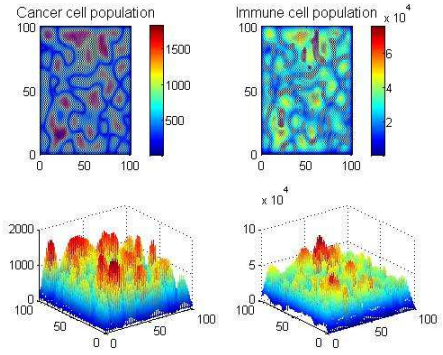

Figure 3: **Turing Patterns of cancer-immune model with Gompertzian growth (2.1) for $d_{11} = 250, d_{12} = -2, d_{21} = 8000, d_{22} = 250, \delta = 0.3$**

From our results related to cross-diffusion on cancer-immune cell population, we hope that it will suggest new empirical and theoretical studies and make a bridge for further study. We believe that theoretical and experimental studies and constructive criticisms will clarify the actual mechanisms that take place in real biological systems.

REFERENCES

Byrne, H. M. (1999a). Using mathematics to study solid tumour growth, in *Proceedings of the 9th General Meetings of European Women in Mathematics*,(1999a) pp. 81-107.

Chambers, A. F. and Werb, Z. (2015). Invasion and metastasis-recent advances and future challenges. *J Mol Med* (Berl). 2015 Apr; 93(4):361-8.

Gierer, A. and Meinhardt, H. (1972). A theory of biological pattern formation*, Kybernetik*, 12, 3039.

Gompertz, B. (1825). On the Nature of the Function Expressive of the Law of Human Mortality, and on a New Mode of Determining the Value of Life Contingencies. *Philosophical Transactions of the Royal Society of London*, Vol. 115. (1825), pp. 513-583.

Gui-Quan, S., Zhen, J., Li, L., Mainul, H. and Bai-Lian, L., (2012). Spatial patterns of a predator-prey model with cross diffusion, *Nonlinear Dyn* (2012) 69:1631-1638 DOI 10.1007/s11071-012-0374-6.

Laird, A. K. (1964). Dynamics of Tumor Growth. *British journal of cancer, 13*(3), 490-502. https://doi.org/10.1038/bjc.1964.55.

Lingeshwaran, S. and Puthur, T. S. (2018). Optimal Control Problem for Cancer Invasion Reaction-Diffusion System*. Numerical Functional Analysis and Optimization*, DOI: 10.1080/01630563.2018.1487453.

Malchow, H., Petrovskii, S. V., and Venturino E., (2008). Spatiotemporal Patterns in Ecology and Epidemiology-Theory,Models, and Simulation*, Mathematical and Computational Biology Series*, Chapman & Hall, Boca Raton, Fla, USA.

Michelle, L. (2012). Perspectives on modelling human growth: Mathematical models and growth biology. *Annals of human biology*. 39. 342-51. 10.3109/03014460.2012.704072.

Tjørve, K. and Tjørve E. (2017). The use of Gompertz models in growth analyses, and new Gompertz-model approach: An addition to the Unified-Richards family. *PLoS ONE 12*(6): e0178691. https://doi.org/10.1371/journal.pone.0178691.

Turing, A. M. (1952). The Chemical Basis of Morphogenesis. *Philosophical Transactions of the Royal Society of London*. Series B, Biological Sciences, Vol. 237, No. 641., pp. 37-72.

WHO (2021, September 21). World Health Organization. https://www.who.int/news-room/fact-sheets/detail/cancer.

Wilkie, K. P. and Hahnfeldt, P. (2013). Mathematical models of immune-induced cancer dormancy and the emergence of immune evasion. *Interface Focus* 3: 20130010. https://royalsocietypublishing.org/doi/10.1098/rsfs.2013.0010.

Wishart, D. S. (2015). Is Cancer a Genetic Disease or a Metabolic Disease? *EBioMedicine*, 2(6), 478-479. doi:10.1016/j.ebiom.2015.05.022.

Zheng, Q. and Jianwei, S. (2014). Turing instability in a gene network with cross-diffusion. *Nonlinear Dyn* 78:1301-1310.